Correspondence to:
X. Feng,
fengxinbin@vip.skleg.cn

Effects of Precipitation on Mercury Accumulation on Subtropical Montane Forest Floor: Implications on Climate Forcing

Xun Wang[1], Wei Yuan[1,2], Zhiyun Lu[3,4], Che-Jen Lin[1,5,6], Runsheng Yin[7], Fen Li[1,2], and Xinbin Feng[1]

[1]State Key Laboratory of Environmental Geochemistry, Institute of Geochemistry, Chinese Academy of Sciences, Guiyang, China, [2]University of Chinese Academy of Sciences, Beijing, China, [3]National Forest Ecosystem Research Station, Ailaoshan, Yunnan, China, [4]Key Laboratory of Tropical Forest Ecology, Xishuangbanna Tropical Botanical Garden,, Chinese Academy of Sciences, Mengla, China, [5]Department of Civil and Environmental Engineering, Lamar University, Beaumont, TX, USA, [6]Center for Advances on Water and Air Quality, Lamar University, Beaumont, TX, USA, [7]State Key Laboratory of Ore Deposit Geochemistry, Institute of Geochemistry, Chinese Academy of Sciences, Guiyang, China

Abstract Processes facilitated by precipitation play an important role on mercury (Hg) accumulation on forest floor and therefore key to Hg cycling in forest ecosystems. Sites along the windward slope of 1,250 to 2,400 m at Mt. Ailao, Southwestern China, have higher precipitation than the leeward slope sites. In this study, measurements of Hg concentration and associated stable isotope composition for soil, fresh, and degraded litterfall samples were made at sites along two slopes of Mt. Ailao to quantify the direct and indirect effects of precipitation on Hg accumulation on forest floor. Higher soil Hg concentrations, larger litterfall Hg depositions, and faster litter decomposition rates were observed on the windward slope (1,250–2,400 m). Data of Hg isotopic signatures suggest that Hg in surface soils is mainly derived from litterfall Hg input. Precipitation enhances litterfall Hg deposition by increasing litter biomass production, reduces litter decomposition rate, facilitates short-term Hg uptake to decomposing litter, and potentially increases microbial activity that increases Hg loss via microbial reduction or runoff. Structural equation modeling results support that the indirect effect of precipitation on increased biomass production merge as the most important factor controlling soil Hg variation. Given the climate forcing on global precipitation pattern and vegetation growth cycle, Hg biogeochemical cycling is likely to continue to evolve under the changing climate.

Plain Language Summary Precipitation has direct and indirect effects on Hg accumulation and transformation on forest floor. The direct effect is that atmospheric Hg enters into forest floor via precipitation, throughfall, and cloud water deposition. In addition, precipitation likely has an indirect effect on Hg accumulation by influencing litter biomass production and postdepositional processes of Hg, such as litter decomposition, Hg reemission, and surface runoff. The objective of this study is to better quantify the direct and indirect effects of precipitation on Hg accumulation on forest floor. The study sites are located along the leeward and windward slopes of Mt. Ailao in Southwest China. Precipitation intensity is the main variable at the same altitude between two slopes. Our results showed that influences from precipitation on soil Hg accumulation are largely through the indirect effects caused by influencing litterfall Hg deposition. We also suggest that the changed precipitation pattern can force variations of litterfall Hg deposition and soil Hg accumulation globally.

1. Introduction

Thirty one percent of terrestrial surface is covered by forest ecosystems (Keenan et al., 2015). Mercury (Hg) processes in forest ecosystems play an important role in global Hg cycling. Elevated atmospheric Hg deposition to montane forest causes a higher risk of accumulation and bioconcentration of MeHg, that is, Methyl Hg (Blackwell & Driscoll, 2015; X. Wang, Luo, et al., 2017; H. Zhang et al., 2013). Mercury enters into forest ecosystems through wet and dry Hg (II) depositions and Hg^0 deposition (i.e., via litterfall and direct deposition to soils). Earlier studies showed that the amount of Hg derived from the atmosphere distinctly increases with altitude and highlighted the importance of greater Hg deposition via precipitation, throughfall, and

cloud water (i.e., direct effects of precipitation) at a higher elevation (Blackwell & Driscoll, 2015; Stankwitz et al., 2012; H. Zhang et al., 2013). However, recent studies suggested that atmospheric Hg^0 deposition is the main source of Hg accumulating within the forest floor, and precipitation likely has an indirect effect on Hg accumulation by influencing litter biomass production (X. Wang, Luo, et al., 2017; Zheng et al., 2016). Precipitation also influences the postdepositional processes of Hg, such as litter decomposition, Hg reemission, and surface runoff (Gustin & Lindberg, 2000; J. Munthe et al., 1995; Rea et al., 2000; X. Wang, Luo, et al., 2017); however, these processes are quite difficult to quantify due to complicated biological, orographic, and climatic influences (Yin et al., 2016; H. Zhang et al., 2013). Thus, the role of precipitation on Hg accumulation on forest floor is still unclear and therefore warrants better investigation.

Data of stable Hg isotopes in environmental samples provide mechanistic insights into biogeochemical cycling of Hg in the environment. Mercury isotopes undergo mass-dependent fractionation (MDF; reported as $\delta^{202}Hg$) and mass-independent fractionation (MIF; reported as $\Delta^{199}Hg$, $\Delta^{200}Hg$ and $\Delta^{201}Hg$), resulting in significant differences in Hg isotopic compositions among environmental pools (Blum et al., 2014). The Hg (II) and Hg^0 in the atmosphere have been shown to have distinct Hg isotopic compositions (Chen et al., 2012; M. Enrico et al., 2016; X. Fu, Maruszak, et al., 2016; Gratz et al., 2010). Atmospheric Hg (II) pool is characterized by positive $\Delta^{199}Hg$, $\Delta^{200}Hg$, and $\Delta^{201}Hg$ values, whereas atmospheric Hg(0) pool has complementary negative Hg isotopic values. The isotopic data serve as useful tools for identifying sources and processes of Hg in forest ecosystems.

The objective of this study is to better understand the role of precipitation on Hg accumulation and transformation in forest ecosystems. The study sites are located along the leeward and windward slopes of Mt. Ailao in Southwest China. Precipitation intensity is the main variable at the same altitude on the two slopes. Measurements of Hg isotopes were utilized to trace Hg sources and biogeochemical processes. To quantify the influence of precipitation, we examined the correlations of precipitation to litterfall Hg input, soil Hg concentration, litter decomposition rate, and Hg mass variation during litter decomposition. Structural equation modeling (SEM) was applied to synthetically assess the direct and indirect effects of precipitation on Hg accumulation in forest soil.

2. Methodology

2.1. Site Description

Mt. Ailao is located at the boundary of Yunan-Guizhou Plateau and Hengduan Mountains in Yunnan province, Southwestern China (Figure S1 in the supporting information). The observed 1.4–2.0 ng/m^3 atmospheric Hg^0 concentration (close to 1.4–1.6 ng/m^3 background value in the northern hemisphere; Sprovieri et al., 2016) at Mt. Ailao suggests limited impact from direct anthropogenic emissions (H. Zhang et al., 2016). From the meteorological data during 1985–2016 (Figure S1), the precipitation increases with the increasing altitude on both slopes. The annual precipitation intensity at 1,000 m (above sea level) of windward slope is about 200 mm higher than that at the same altitude level of leeward slope ($p < 0.01$, by Independent Samples T test). Such precipitation difference becomes smaller with the increasing altitude until comparable annual precipitation intensities at the mountain top (2,500 m, above sea level). Air temperature at the same altitude level of two slopes are similar (Figure S1).

Mt. Ailao has a distinct vegetation structure with respect to its altitude. The forest age, canopy coverage, forest type, and dominant tree species of the study sites are summarized in Table S1 and Figure S1. Briefly, dry-hot valley vegetation predominates on leeward slope at 800–1,000-m altitude; coniferous forests (mainly pinus spp.) mixed with evergreen broadleaf species (<40%) on both slopes at 1,000–2,400 m; and evergreen broadleaf species on both slopes at >2,500 m. The forest soil is mainly Luvisol with soil pH of 4.4–4.9 (Z. Yang & Yang, 2011).

2.2. Sampling

Nine sites on the leeward slope (850, 1,000, 1,250, 1,500, 1,850, 2,100, 2,400, 2,500, and 2,650 m) and seven sites on the windward slope (1,250, 1,500, 1,850, 2,100, 2,400, 2,500, and 2,650 m) were selected for sampling. At each site, five 5 × 5 m subplots were established for sample collection, following a previous protocol (X Wang, Luo, et al., 2017). Zero to ten centimeters of surface soil sample for each subplot were collected in April 2016. We randomly selected three out of five subplots at each site to collected monthly litterfall

samples. Monthly litterfall samples were collected since January 2017, by 1 m × 1 m nylon nets hanging at 0.3 m above ground, following our previous methods (X. Wang, Lin, et al., 2016). Overall, we totally collected 80 surface soil samples (16 sites × 5 replicates) and 576 monthly litterfall samples (16 sites × 3 replicates × 12 months).

We conducted the 1-year litter decomposition experiment, following the procedure described in our previous work (X. Wang, Lin, et al., 2016). Briefly, 15 g of a well-mixed litter sample was placed in a 15 cm × 15 cm nylon bag that had 1 mm × 1 mm mesh size. We totally put 240 litter bags at 16 sites (i.e., 15 bags for each site), and each of 48 bags of samples (16 sites×3 replicates) was collected starting from 0, 3, 6, 9, and 12 months after 25 January 2017.

2.3. Concentration Measurements

In this study, vegetation samples were dried in an oven at 60 °C for 48 hr until <0.03% of mass variation occurred in 8 hr. Soil samples were air dried at a dark and clean room and then ground in an agate mortar and sieved by a 200-mesh sieve (74 μm). The reason for using air drying is that the loss or increase of Hg mass caused by the air-soil flux exchange during 1- or 2-week time of natural air drying would not significantly influence soil Hg concentration, and the difference of Hg concentration between by air drying and freeze drying is low ≤5% (average = $1.9 \pm 1.5\%$, 1SD, and $n = 5$; by preexperiment). Hg concentrations of litter and soil samples were measured by Lumex RA-915+ Direct Mercury Analyzer (X. Wang, Lin, et al., 2016). Standard reference materials were measured in every 10 samples, which yielded recoveries of 95–105%. GBW07405 (GSS-5, 290 ± 40 ng/g) was used as the soil Hg standard. GBW10020 (GSB-11, Hg = 150 ± 25 ng/g) and GBW10049 (GSB-27, Hg = 12 ± 3 ng/g) were used as the litter Hg standard.

The decomposition rate was calculated using a first regression model (i.e., decomposition rate defined by first-order kinetics; Breymeyer et al., 1997; Harmon et al., 2009):

$$M_t = M_0 \times e^{-(k_d \times t)}, \tag{1}$$

where M_t is the present litter mass remaining, M_0 is the initial litter mass, t is time in month, and k_d is the decomposition rate constant in month. Table S2 shows M_t / M_0 at each site during 1-year litter decomposition. We used MATLAB to obtain the k_d in equation (1). Hg mass variation (V_{Hg}) during litter decomposition is estimated as

$$V_{Hg} = (Hg_0 - Hg_f)/Hg_0 \times 100\%, \tag{2}$$

where Hg_0 is the initial Hg mass in litter, and Hg_f is the final Hg mass in litter remaining during 1-year decomposition. $V_{Hg} > 0$ means Hg mass loss after 1-year litter decomposition, while $V_{Hg} < 0$ means Hg mass increase.

2.4. Isotopes Measurements

Four random samples collected in January, April, August, and October (one in each month) at each site were mixed to make a composite sample. The Hg isotopic signatures of the litterfall and soil composite samples were determined by using a method that has been described previously (X. Wang, Luo, et al., 2017). Briefly, all samples were processed by a double-stage tube furnace and trapping solutions (anti aqua regia, HNO_3:HCl = 2:1, v/v) for Hg preconcentration, and the Hg solutions were diluted to 1 ng/ml prior to Hg isotope measurement by the Nu II Plasma mass spectrometer (MC-ICP-MS, Nu Instruments, UK). The acid strength of each diluted solution was 8–12%. The recoveries of preconcentrating were both 95% to 105% for BCR-482 (reference standard for litter samples), GSS-4 (590 ± 50 ng/g, reference standard for soil samples), and samples. The sample introduction system for Hg isotope ratio measurements consists of an online Hg vapor generation system (Yin et al., 2010; HGX-200, Teledyne CETAC Technologies, USA) coupled to a CETAC Ardius 2 Desolvating Nebulizer System. The SnCl2 (3%) was used as the reducing agent for Hg and mixed online with Hg standards or samples to generate Hg^0. Instrumental mass bias correction was accomplished using NIST SRM 997 as an internal standard and external standard-sample bracketing with a NIST SRM 3133 Hg solution. Mercury concentrations in acid matrices of Hg standard solutions (NIST-3133) and UM-Almadén secondary standard solution were matched to the sample solutions (1 ppb, 10% acid strength

Table 1
Pearson Correlation Coefficients Among Precipitation (n = 16), Soil Hg Concentration (n = 16), Litterfall Hg Deposition (LBF, n = 16), Litterfall Biomass Production (LB, n = 16), T (Temperature, n = 16), k_d (Decomposition Rate Constant in Month, n = 16), V_{Hg} (Hg Mass Variation During Litter Decomposition, n = 15), $\delta^{202}Hg\_S$ ($\delta^{202}Hg$ in Soil, n = 16), $\Delta^{199}Hg\_S$ ($\Delta^{199}Hg$ in Soil, n = 16), $\Delta^{200}Hg\_S$, ($\Delta^{200}Hg$ in Soil, n = 16), $\delta^{202}Hg\_L$ ($\delta^{202}Hg$ in Litterfall, n = 16), $\Delta^{199}Hg\_L$ ($\Delta^{199}Hg$ in Litterfall, n = 16), and $\Delta^{200}Hg\_L$ ($\Delta^{200}Hg$ in Litterfall, n = 16)

	Precipitation	SoilHg	LBF	LB	k_d	V_{Hg}	T	$\delta^{202}Hg\_L$	$\Delta^{199}Hg\_L$	$\Delta^{200}Hg\_L$	$\delta^{202}Hg\_S$	$\Delta^{199}Hg\_S$	$\Delta^{200}Hg\_S$
Precipitation	1.00												
SoilHg	0.73**	1.00											
LBF	0.56*	0.83**	1.00										
LB	.59*	0.74**	0.84**	1.00									
k_d	−0.47	−0.25	−0.11	0.03	1.00								
V_{Hg}	−.85**	−0.56*	−0.59*	−0.73**	0.49	1.00							
T	−.97**	−0.72**	−0.52*	−0.46	0.64*	0.78**	1.00						
$\delta^{202}Hg\_L$	−0.11	−0.06	−0.32	−0.30	0.03	0.30	0.09	1.00					
$\Delta^{199}Hg\_L$	−0.47	−0.21	−0.12	−0.05	−0.06	0.28	0.47	−0.03	1.00				
$\Delta^{200}Hg\_L$	−0.06	0.07	0.03	0.11	0.11	0.03	0.12	0.66**	0.24	1.00			
$\delta^{202}Hg\_S$	−0.42	−0.42	0.00	0.12	0.56*	0.13	0.55*	−0.05	0.37	0.13	1.00		
$\Delta^{199}Hg\_S$	−.63**	−0.45	−0.12	−0.23	0.29	0.40	0.63**	0.04	0.43	0.01	0.70**	1.00	
$\Delta^{200}Hg\_S$	0.27	0.24	0.18	0.07	−0.04	−0.17	−0.24	0.13	−0.37	−0.31	−0.10	0.02	1.00

**Significant correlation at 0.01 level (two-tailed test). *Significant correlation at 0.05 level (two-tailed test).

in anti-aqua regia solution). The Hg-MDF is reported in δ notation using the unit of permil (‰) referenced to the neighboring NIST-3133 solution:

$$\delta^{202}Hg\ (‰) = 1,000 \times \left[\left(^{202}Hg/\ ^{198}Hg_{sample} \right) / \left(^{202}Hg/\ ^{198}Hg_{NISTSRM3133} \right) - 1 \right]. \quad (3)$$

MIF is reported as $\Delta^{xxx}Hg$ following the convention suggested by Blum and Bergquist (2007):

$$\Delta^{199}Hg\ (‰) = \delta^{199}Hg - 0.2520 \times \delta^{202}Hg, \quad (4)$$

$$\Delta^{200}Hg\ (‰) = \delta^{200}Hg - 0.5024 \times \delta^{202}Hg, \quad (5)$$

$$\Delta^{201}Hg\ (‰) = \delta^{201}Hg - 0.7520 \times \delta^{202}Hg. \quad (6)$$

UM-Almadén secondary standard solution was analyzed for every 10 samples. To assess if the nonunity recoveries resulting from the double-stage offline combustion-trapping technique induced discernible isotopic bias, we measured BCR 482 and GSS-4 at the beginning of sample preconcentration sessions. Results of UM-Almadén ($\delta^{202}Hg = -0.53 \pm 0.04‰$, $\Delta^{199}Hg = -0.00 \pm 0.04‰$, $\Delta^{201}Hg = -0.03 \pm 0.02‰$, Mean $\pm$ 1SD, Standard deviation, $n = 10$) and BCR-482 ($\delta^{202}Hg = -1.65 \pm 0.06‰$, $\Delta^{199}Hg = -0.56 \pm 0.05‰$, $\Delta^{200}Hg = -0.01 \pm 0.03‰$, $\Delta^{201}Hg = -0.58 \pm 0.04‰$, Mean $\pm$ 1SD, $n = 5$), and GSS-4 ($\delta^{202}Hg = -1.70 \pm 0.08‰$, $\Delta^{199}Hg = -0.35 \pm 0.03‰$, $\Delta^{201}Hg = -0.31 \pm 0.03‰$, $\Delta^{200}Hg = -0.00 \pm 0.02‰$, Mean $\pm$ 1SD, $n = 5$) are consistent with recommended values (Blum & Bergquist, 2007; Estrade et al., 2010).

2.5. Statistical Methods

Independent sample t test was utilized to analyze the statistical difference during the site-to-site comparison at the same altitude (e.g., site at 1,250 of windward slope versus site at 1,250 of leeward slope). Paired sample t test was used for determining whether the data means observed on the windward and leeward slopes are significantly different. One-Way ANOVA (Analysis of Variance) was utilized to analyze statistical differences among the means of three or more groups (e.g., Hg isotopic compositions from different plant species). The statistical significance of r is determined at 95% confidence interval by two-tailed tests (Table 1). Multiple Linear Regression (MLR) is used to model the relationship between the explanatory and response variables. Principal component analyses (PCAs) was conducted to explain the variation of soil Hg concentration and soil $\delta^{202}Hg$. Kaiser-Meyer-Olkin and Bartlett's sphericity tests were performed to evaluate how suited the data are for PCAs (Kaiser-Meyer-Olkin should be >0.60). Varimax was used as the rotation method in PCA analyses. All statistical analyses were performed by SPSS version 17.

Based on our hypothesis and available data, a conceptual SEM was constructed to quantify effects of precipitation on Hg accumulation on forest floor. Model construction procedures involved the three stages. First, hypothesized mechanisms for interpretations across precipitation, litterfall Hg deposition, litter decomposition, and soil Hg were proposed in Table S2. Second, PCA was performed to create a multivariate functional index to represent the long-term precipitation effect on soil Hg (details in section 3.4). All variables were standardized into Z scores. Finally, SEM was developed from the conceptual model using χ^2 tests with maximum likelihood estimation. Model fitting was performed by using the Amos software version 24. From the SEM path network, the standardized path coefficient (β) represents the direct effect of one variable on another, and the indirect effect (e.g., one variable affects another variable which in turn affects a third) can be calculated as
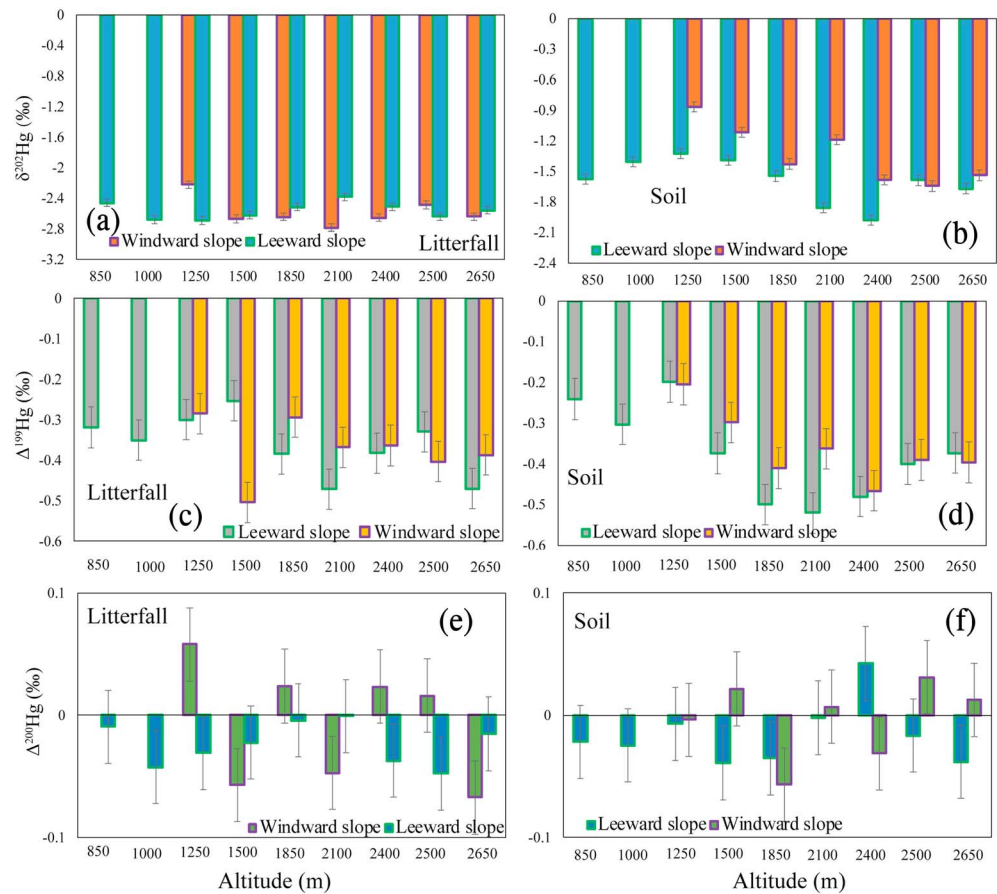
Figure 1. Variations of : (a) δ^{202}Hg in litterfall, (b) δ^{202}Hg in 0—10-cm surface soil, (c) Δ^{199}Hg in litterfall, (d) Δ^{199}Hg in 0—10-cm surface soil, (e) Δ^{200}Hg in litterfall, (f) Δ^{200}Hg in 0—10-cm surface soil along with altitude on leeward and windward slopes of Mt. Ailao. The error bar is 1 standard deviation. The raw data can be found in Table S8.

$$\text{Indirect effect} = \beta_1 \times \beta_2 \times \beta_3 \times \cdots \times \beta_n. \tag{7}$$

3. Results and Discussion

3.1. Dominant Source for Hg Accumulation on Forest Floor

The means of Hg isotopic composition in litter samples (δ^{202}Hg $= -2.51 \pm 0.15‰$, Δ^{199}Hg $= -0.35 \pm 0.07‰$, Δ^{200}Hg $= -0.02 \pm 0.02‰$, 1SD, $n = 16$ sites, Figures 1a, 1c, and 1e) are comparable to these reported for litter or mature leaves in remote forest ecosystems (M. Enrico et al., 2016; M. Jiskra et al., 2015; X. Wang, Luo, et al., 2017; Zheng et al., 2016). Hg isotopic compositions in litter show a weak yet consistent elevation gradient (i.e., $r^2 < 0.2$, $p > 0.05$, Table S4), but there is no clear difference between the data observed on both slopes ($p > 0.05$, Figures 1a, 1c, and 1e and Table S5). The study site is far away from the location of known anthropogenic sources. Mercury in litter at this site is mainly from long-range transport and therefore shares similar Hg isotopic signatures on both slopes at same altitude. The Hg isotopic compositions are also quite consistent for different plant species ($p > 0.05$, One-Way ANOVA test), suggesting that Hg isotopes undergo similar fractionation processes during the uptake of Hg. Similarly, soil samples (Figures 1b, 1d, and 1f) show negative δ^{202}Hg ($-0.148 \pm 0.27‰$, $n = 16$ sites), negative Δ^{199}Hg ($-0.36 \pm 0.10‰$, $n = 16$ sites), and Δ^{200}Hg of ~0 ($-0.01 \pm 0.04‰$, $n = 16$ sites). Soil Δ^{199}Hg decreases with the increase of altitude (r ranges -0.86 to -0.60, $p < 0.05$, Table S4). Interestingly, the windward slope sites at <2,500 m have more positive δ^{202}Hg (0.1–0.7‰ shift) than leeward slope sites ($p < 0.05$, on slope-slope level, Table S5).

The MIF signatures of Hg isotopes are unlikely to be altered by postdepositional processes as seen for MDF in forest ecosystems, making the MIF signatures of Hg a useful tracer to identify specific sources (Blum et al.,
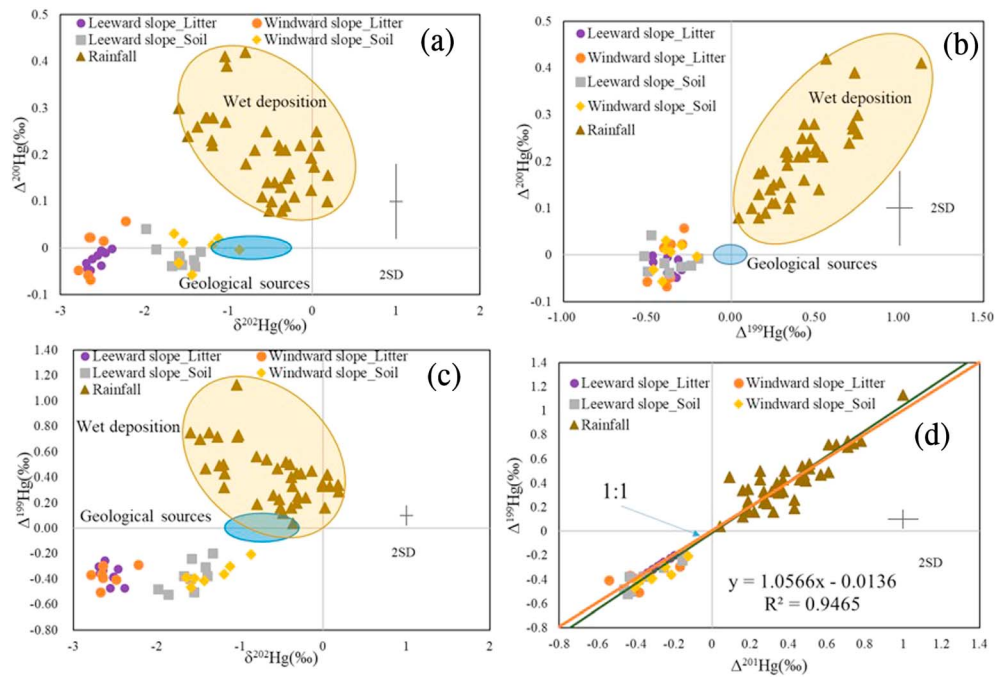
Figure 2. Relationships among (a) $\Delta^{200}Hg$ versus $\delta^{202}Hg$, (b) $\Delta^{200}Hg$ versus $\Delta^{199}Hg$, (c)$\Delta^{199}Hg$ versus $\delta^{202}Hg$, (d)$\Delta^{199}Hg$ versus $\Delta^{201}Hg$. The Hg isotopic signatures for geological Hg are derived from literatures (Blum et al., 2014; Smith et al., 2008) and for wet deposition from literatures (Chen et al., 2012; Demers et al., 2013; Gratz et al., 2010; Sherman et al., 2012; Yuan et al., 2015).

2014; Sonke, 2011; X. Wang, Luo, et al., 2017). There are two possible pathways that can induce the odd-MIF (i.e., $\Delta^{199}Hg$ and $\Delta^{201}Hg$) of soil Hg: One is Hg^0 reemission by photoreduction with magnetic isotope effect, and the other is dark reduction by natural organic matter, which is associated with the nuclear volume effect (M. Enrico et al., 2016; M. Jiskra et al., 2015; X. Wang, Luo, et al., 2017; Zheng et al., 2016). Photochemically induced Hg^0 reemission in forest floor is typically not important because of shading by the dense forest canopy (Agnan et al., 2016; X. Wang, Luo, et al., 2017; X. Wang, Yuan, et al., 2017). The scatter plot of $\Delta^{199}Hg$ versus $\Delta^{201}Hg$ yields a slope of ~1.0 (Figure 2d), suggesting negligible nuclear volume effect ($\Delta^{199}Hg:\Delta^{201}Hg \sim 1.6$; Blum et al., 2014; Jiskra et al., 2015). The positive $\Delta^{200}Hg$ signal is mainly observed in precipitation and during Hg^0 oxidation processes ^{200}Hg MIF (Blum et al., 2014; Chen et al., 2012; Sun et al., 2016). Data from rainfall samples collected at global sites show that Hg in precipitation of remote sites has a consistently different isotopic signatures from those found in litter and soil samples (Figures 2a–2d; Chen et al., 2012; Demers et al., 2013; Gratz et al., 2010; Sherman et al., 2012; Yuan et al., 2015). Therefore, the positive $\Delta^{199}Hg$ and $\Delta^{200}Hg$ in precipitation can be treated as a unique atmospheric Hg (II) input endmember (Blum et al., 2014; Chen et al., 2012; Demers et al., 2013; Maxime Enrico et al., 2017; M. Enrico et al., 2016; Gratz et al., 2010; D. Obrist et al., 2017; Yu et al., 2016).

Precipitation intensity at 2,650 m regions is nearly 2 times higher than at 850 m. However, $\Delta^{200}Hg$ values in all surface soil are ~0 (-0.01 ± 0.04‰, $n = 16$). In addition, $\Delta^{199}Hg$ of surface soils are much negative than that of precipitation (-0.36 ± 0.10‰ vs. 0.44 ± 0.23‰ in Figures 3b and 3c) but close to that of litterfall. This suggests that litterfall Hg deposition is the main source for soil Hg accumulation. Geological Hg, derived from weathering of bed rocks, has been shown to have less negative $\delta^{202}Hg$ (-0.6‰ to -1.5‰, Figure 3a) without significant MIF of ^{199}Hg and ^{200}Hg (Figures 3a–3c; Blum et al., 2014; Smith et al., 2008). The mixing of geological Hg may contribute Hg to soil for samples collected at <1,850-m sites, which showed more positive soil $\delta^{202}Hg$ and $\Delta^{199}Hg$ values (Figures 1b and 1d). Overall, isotopic evidence suggests that litterfall input is the dominant source for Hg found in surface soil, consistent with results from China Tibetan forests (X. Wang, Luo, et al., 2017) and U.S. forests (Zheng et al., 2016). The annual average of Hg concentration in precipitation of Mt. Ailao is 4.9 ± 3.1 ng/L (X. Wang, Lin, et al., 2016), yielding wet deposition of 4–10 $\mu g \cdot m^{-2} \cdot year^{-1}$ at the study sites. The litterfall Hg input is 2–4 times higher than wet deposition
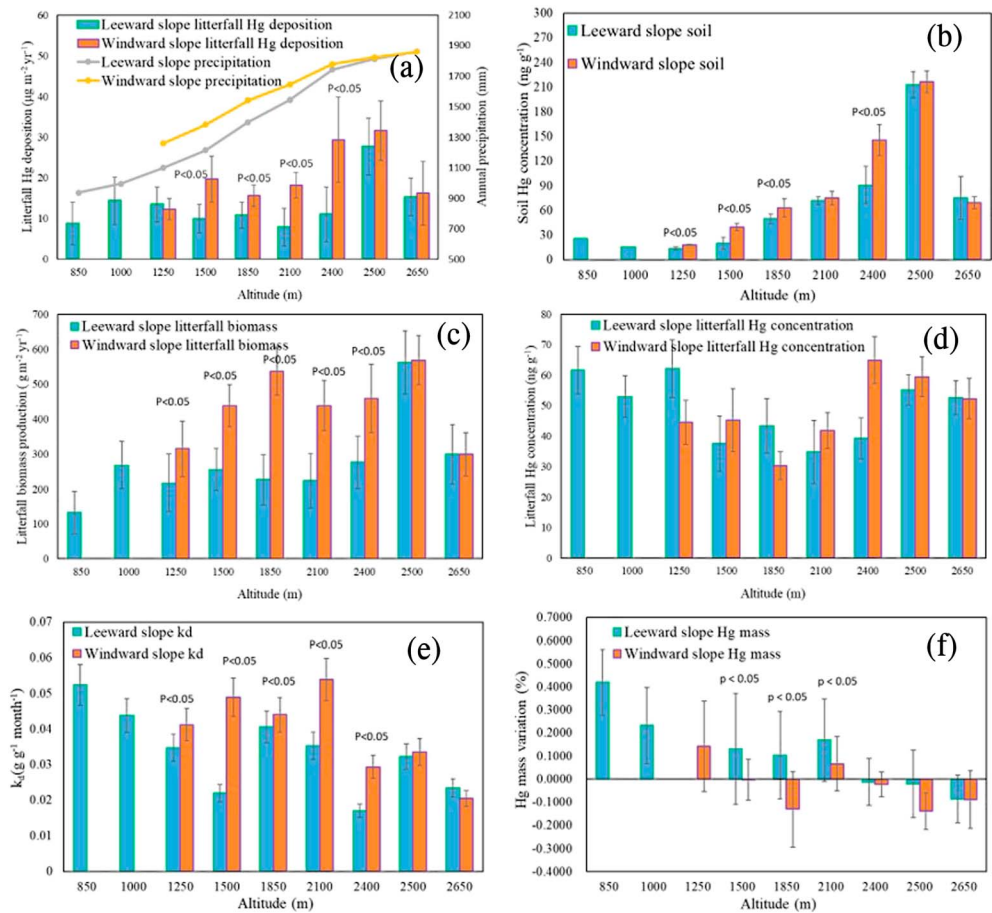
Figure 3. (a–d) Variations of annual precipitation, litterfall Hg deposition, Hg concentration in 0–10 cm surface soil, litterfall biomass production, and litterfall Hg concentration; (e and f) variations of k_d and V_{Hg} (Hg mass during 1-year litter decomposition) along with altitude on leeward and windward slopes of Mt. Ailao. The error bar is 1 standard deviation. The raw data can be found in Table S9.

(Figure 3a). Moreover, surface soil Hg concentration is significantly correlated to litterfall Hg input ($r^2 = 0.69$, $p < 0.01$, Figure S2). This, again, points to litterfall Hg being the primary source of Hg in soil.

PCA in Table 2 shows that the sampling locations on the two slopes (PC1, 46% variances of soil Hg) and elevation (PC2, 24% variances of soil Hg) influence soil Hg concentration. Soil Hg concentrations along the windward slope of 1,250, 1,500, 1,850, and 2,400 m are significantly higher than the values on the leeward slope of the same altitude ($p < 0.05$, on site-site level, Figure 3b). Figure 3b shows that Hg concentration in surface soil on both slopes significantly increases ($p < 0.05$, two-tailed t test, Table S4) from 850 to 2,500 m and sharply decreases at 2,650 m. PC1 and PC2 both have high factor loadings for variables representing influences from litterfall Hg deposition (i.e., litterfall Hg deposition and litterfall biomass production in PC1; $\Delta^{199}Hg$ of soil Hg in PC2). High factor loadings for variables related to litter decomposition (i.e., k_d and V_{Hg}) in PC1 and PC2 were also identified, suggesting the importance of litter decomposition. High factor loadings for precipitation and temperature were observed in both PC1 and PC2, indicating that the two factors impose strong indirect effects on soil Hg by influencing litterfall Hg deposition and litter decomposition processes.

3.2. Effect of Precipitation on Litterfall Hg Deposition

Figure S3 shows that the monthly litterfall Hg input is highly correlated to the litterfall biomass production ($r^2 > 0.70$, $n = 576$ samples) rather than to the Hg concentration in litterfall ($r^2 < 0.20$, $n = 576$ samples), suggesting that the variation of litterfall Hg deposition is controlled by litter biomass production,

Table 2
Using PCAs to Explain Variations of Soil Hg Concentration

	PCA component (78% variances explained)	
Variable	PC1 (54%)	PC2 (24%)
SoilHg	**0.681**	**−0.487**
LBF	**0.878**	−0.103
Precipitation	**0.661**	**−0.698**
Temperature	**−0.533**	**0.805**
Δ^{199}Hg_S	−0.044	**0.805**
Slope	**0.759**	0.390
LB	**0.926**	−0.004
Altitude	**0.548**	**−0.800**
k_d	−0.064	**0.744**
V_{HG}	**−0.779**	**0.447**
δ^{202}Hg_S	0.231	**0.871**

Note. LBF is litterfall Hg deposition, Δ^{199}Hg_S is Δ^{199}Hg of soil Hg, LB is litterfall biomass production, and δ^{202}Hg_S is δ^{202}Hg of soil Hg. KMO value = 0.674. Slope = 1 for leeward site and =2 for windward site in PCAs. PCA = principal component analysis. Number in bold font means the significant factor loading.

consistent with earlier results (X. W. Fu, Yang, et al., 2016; X. Wang, Bao, et al., 2016). MLR analysis (Table S6) shows that precipitation and temperature predominantly influence litter biomass production ($r^2 = 0.58$, Table S6), showing greater production with respect to higher precipitation and temperature. Annual precipitation intensity at site of 1,250, 1,500, 1,850, 2,100, and 2,400 m of windward slope (Figure S1) is significantly higher than that at the same altitude levels of leeward slope ($p < 0.05$, both on site-site and slope-slope level, Table S5), while the temperature on both slopes is comparable ($p > 0.05$, both on site-site and slope-slope level, Table S5). This supports the precipitation effect on litterfall Hg deposition through enhancing litter biomass production.

Figures 3a and 3c show that the litterfall Hg deposition and litterfall biomass production along the windward slope of 1,500, 1,850, 2,100, and 2,400 m are both significantly higher than the values on the leeward slope of the same altitude ($p < 0.05$, both on site-site and slope-slope level, Figures 3a and 3c and Table S5). However, Hg concentration in litter samples shows little difference between two slopes ($p > 0.05$, Figure 3d and Table S5). Greater litterfall Hg deposition on the windward slope site of 1,250 m (Figure 3a) was not observed because of the much higher litterfall Hg concentration at leeward site of 1,250 m (66 ± 9 ng/g vs. 44 ± 7 ng/g, Figure 3c). The observed differences of litterfall biomass production and litterfall Hg deposition are not caused by vegetation type, since sites at the same altitude have similar vegetation types (Figure S1 and Table S1) and forest ages (Table S1). Tables 1 and S6 both suggest that precipitation as the most important factor to explain 35% variances of litterfall biomass production.

The above analysis clearly show that the precipitation plays an important role in Hg accumulation in forest top soil through enhancing the production of vegetative biomass. Higher soil Hg concentration was observed at the windward sites at 1,250, 1,500, 1,850, and 2,400 m (Figure 3b). Table 1 also shows that precipitation is significantly correlated to soil Hg concentration, to litterfall Hg deposition and to litterfall biomass production (all $r > 0.50$, $p < 0.05$ by two-tailed test). Interestingly, a significantly negative correlation between precipitation and Δ^{199}Hg in surface soil was found ($r = −0.63$, $p < 0.01$, Table 1). Figures 2b and 2c show positive Δ^{199}Hg in precipitation samples, which rules out precipitation as the main source for soil Hg. Instead, Hg in surface soil shows negative Δ^{199}Hg, similar to litterfall Hg. This indicates that the effect of precipitation is indirect through promoting vegetative biomass production.

3.3. Precipitation Effects on Litter Decomposition

The values of k_d (litter decomposition rate constant) are significantly different on the two slopes, higher k_d along the windward slope of 1,250 to 2,400 m than on the leeward slope of the same altitudes ($p < 0.05$, both on site-site and slope-slope level, Figure 3e and Table S5). In addition, we observed a decreasing elevation gradient for k_d on both slopes ($p < 0.05$, Table S4). The global meta-analysis suggests that higher temperature and precipitation induce a faster k_d (D. Zhang et al., 2008). In this study, MLR analysis shows that temperature plays a more important role than precipitation in controlling the elevation gradient of k_d (Table S6). However, the different k_d along the two slopes is mainly induced by precipitation. We found significantly lower V_{Hg} (Hg mass variation during 1-year litter decomposition, positive value for Hg loss while negative value for Hg increase) at the sites of 1,500, 1,850, and 2,100 m of windward slope (Figure 3f). However, a poor correlation between V_{Hg} and k_d ($r^2 = 0.19$, $p > 0.05$ by two-tailed test) was found, suggesting litterfall decomposition rate would not significantly influence Hg mass variation during 1-year litter decomposition. Interestingly, V_{Hg} is positive for sites at <2,400 m and negative for sites at 2,400–2,650 m on both slopes. Such shifts of V_{Hg} suggest a loss of Hg mass at lower altitudes but an increase at higher altitudes. Two possible reason can explain the Hg loss during litter decomposition at lower altitudes. One is Hg^0 evasion due to the C and N microbial mineralization during litter decomposition (D. Obrist et al., 2010; Pokharel & Obrist, 2011; Strauss et al., 2012). The other is Hg leaching with the formed dissolved organic carbons (Pokharel & Obrist, 2011; X. Wang, Lin, et al., 2016).

Table 3

Using PCAs to Explain Variations of $\delta^{202}Hg$ of Soil Hg, $\delta^{202}Hg\_S$ is $\delta^{202}Hg$ of Soil Hg, and $\delta^{202}Hg\_L$ is $\delta^{202}Hg$ of Litter Hg

	PCA component (79% variances explained)	
Variable	PC1 (53%)	PC2 (26%)
$\delta^{202}Hg\_S$	**0.697**	**0.555**
Precipitation	**−0.907**	**0.484**
k_d	**0.717**	0.419
Temperature	**0.968**	−0.216
Slope	0.003	**0.944**
Altitude	**−0.957**	0.252
$\delta^{202}Hg\_L$	0.089	−0.274

Note. KMO value = 0.681. Slope = 1 for leeward site and =2 for windward site in PCAs. Number in bold font means the significant factor loading.

We observed ~40% Hg mass loss at 850 m, while ~10% Hg mass increment at 2,650 m. MLR analysis shows that precipitation explains 71% V_{Hg} variability ($r = −0.85$, $p < 0.01$, Table S6), suggesting Hg uptake by decomposing litter during litter decomposition, particularly at higher altitudes. Atmospheric Hg^0 uptake by decomposing litter and deep soil Hg mixing by fungal translocation are possible causes for such Hg mass increase (Demers et al., 2007; X. Wang, Lin, et al., 2016). However, both pathways cannot explain the strong correlation between precipitation and V_{Hg} (Hg mass variation during the 1-year litter decomposition).

A more plausible explanation is that the Hg source of uptake by decomposing litter is from throughfall (Demers et al., 2007; Pokharel & Obrist, 2011; X. Wang, Lin, et al., 2016). However, Hg isotopic signatures in throughfall samples have not been reported. Hg in throughfall has been proposed to originate from particulate-bounded Hg (PBM) and gaseous-oxidized Hg (GOM) washed off from leaf surfaces during rainfall events (D. F. Grigal, 2003; Rea et al., 1996; Rea et al., 2001). PBM at remote sites has similar $\delta^{202}Hg$ and $\Delta^{199}Hg$ compared to rainfall samples but with ~0 $\Delta^{200}Hg$ (Yu et al., 2016). The GOM MIF signatures at remote forest sites is not yet understood. Only one study reported GOM MIF signatures in a coastal environment ($\Delta^{199}Hg$: −0.28‰ to 0.18‰ and $\Delta^{200}Hg$: 0.08‰ to 0.28‰; Rolison et al., 2013). The contribution of MIF signatures from PBM and GOM may shift the MIF signals in throughfall. Photoreduction of deposited Hg (i.e.,PBM and GOM) at the surface of foliage (Demers et al., 2013; Zheng et al., 2016), mixing of Hg MIF signatures with biomass of tree detritus and epiphytes (e.g., bark, lichen, and moss, negative $\Delta^{199}Hg$ and ~0 $\Delta^{200}Hg$, can also deviate Hg MIF signatures in throughfall samples from precipitation; M. Enrico et al., 2016; Daniel Obrist et al., 2018). Further studies on isotope compositions of throughfall help fully assess the contribution of throughfall Hg in soil Hg accumulation.

X. Wang, Lin, et al. (2016) reported ~5% Hg mass increment during 2-year litter composition at a nearby site at 2,450 m. In this study, ~1% to ~14% of Hg mass increase was observed during litter decomposition at sites of 2,400 and 2,500 m during 1 year. Although the short-term (1–2 years) decomposition period does not infer long-term accumulation trend, the continual coverage of newly deposited litter can block external Hg uptake by the decomposing litter underneath (X Wang, Lin, et al., 2016) and possibly cause Hg loss in the decomposing litter through C and N mineralization. Reemission of Hg^0 by biologically mediated reduction can lead to a positive shift of $\delta^{202}Hg$ on forest floor without significant MIF (M. Jiskra et al., 2017, 2015; Kritee et al., 2007, 2009; Woerndle et al., 2018). The more positive $\delta^{202}Hg$ (~1–1.5‰ shift) in surface soil than in fresh litter confirms such Hg loss during long-term litter decomposition mediated biologically because of negligible MIF shifts (Figures 1a–1d). Similar $\delta^{202}Hg$ shifts were observed in forests of North America (up to 1.3‰) and Europe (0.4‰; M. Jiskra et al., 2015; Zheng et al., 2016).

Table 1 shows a significantly positive correlation between k_d and $\delta^{202}Hg$ of soil Hg ($r = 0.56$, $p < 0.05$), suggesting that the higher litter decomposition rate finally leads to a more positive $\delta^{202}Hg$ of soil Hg. Using PCAs, we obtained two primary components (PC1 and PC2) in Table 3. PC1 mainly represents the elevation gradient that higher elevation induces a lower temperature, slower k_d, higher precipitation, and more negative $\delta^{202}Hg$ in soil (49% variances of soil $\delta^{202}Hg$ explained by PC1). It is noteworthy that temperature has the highest factor loading in Table 3. The higher temperature can lead to a faster litter decomposition rate ($r = 0.64$, $p < 0.05$, Table 1) and larger soil Hg reemission (Agnan et al., 2016), thus inducing more positive $\delta^{202}Hg$ in surface soil ($r = 0.55$, $p < 0.05$, Table 1). PC2 mainly represents the "slope effect" that yields more positive $\delta^{202}Hg$ of soil Hg for the windward slope sites at 1,250 to 2,400 m (Figure 1b). As discussed, temperature is comparable between two slopes at the same altitude, but precipitation is significantly higher on windward slope. Greater incorporation of geogenic sources (geogenic sources with more positive $\delta^{202}Hg$ and ~0 $\Delta^{199}Hg$ in Figures 2b and 2c) on windward slope cannot solely explain the difference observed along the two slopes because contribution from geogenic sources will also give a more positive $\Delta^{199}Hg$ in soil sample, which was not significantly observed on the windward slope ($p > 0.05$, on slope-slope level, Figure 2d and Table S6). Another cause is likely that the long-term effect of higher precipitation induced soil Hg reemission during litter decomposition. This is verified in Table 3 that positive factor loadings of k_d,
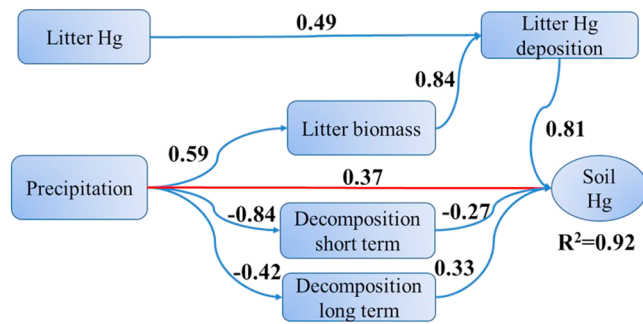
Figure 4. Structural equation modeling fitted to soil Hg concentration among litterfall Hg concentration, precipitation, litterfall biomass, litterfall Hg deposition, and short-term and long-term litterfall decompositions. Numbers adjacent to arrows represent the standardized path coefficients. R^2 indicates the proportion of variance explained. The red arrow represents the direct effect of precipitation (i.e., wet Hg deposition) on soil Hg.

precipitation, and δ^{202}Hg of soil Hg (31% variances of δ^{202}Hg of soil Hg explained by PC2). We recommend a further long-term litter decomposition study to verify our hypothesis.

3.4. Results From SEM Modeling

Precipitation can induce additional Hg uptake from environment by decomposing litter (likely from throughfall). We used V_{Hg} (Hg mass variation during 1-year litter decomposition) to represent this short-term effect of precipitation. We used the PCA component 1 (explaining 60% of total variances, Table S7) of δ^{202}Hg in soil, the shift of δ^{202}Hg between litterfall and soil, and k_d to represent the long-term effect induced by precipitation. Precipitation intensity can infer the wet Hg deposition variations as earlier studies suggest that variation of seasonal or spatial wet Hg deposition is controlled by the precipitation intensity (X. W. Fu, Yang, et al., 2016; Sprovieri et al., 2017; X. Wang, Lin, et al., 2016).

SEM pathway network in Figure 4 explains 92% variances of Hg concentration in soil. The negative standardized path coefficient between precipitation and short-term litter decomposition means that a lower precipitation leading to a smaller Hg mass increase. The negative standardized path coefficient between precipitation and long-term litter decomposition means that the higher precipitation increasing Hg loss via microbial reduction or runoff. The SEM further confirms that litterfall biomass is the primary factor controlling the variation of litterfall Hg deposition (direct effect: 0.84), and the litterfall Hg deposition shapes the variation of Hg concentration in soil (direct effect: 0.81). The direct effect of precipitation on soil Hg concentration is 0.37. The highest indirect effect of precipitation soil Hg concentration is by influencing litterfall Hg deposition (indirect effect: 0.40), followed by short-term litter decomposition (indirect effect: 0.23), and then by long-term litter decomposition (indirect effect: −0.14). The SEM pathway network suggests that influences from precipitation on soil Hg accumulation are largely through the indirect effects caused by of precipitation on litterfall Hg deposition.

4. Implications

Recent studies suggested a Hg distribution defined by land cover and water-limited plant productivity via the analysis of correlations among soil Hg concentration, leaf area index, and Hg/C ratios (D. Obrist et al., 2016; X. Wang, Luo, et al., 2017; Zheng et al., 2016). We combined comprehensive field observations and Hg isotopic signatures along with windward and leeward slopes of Mt. Ailao to further determine the contribution of precipitation on Hg accumulation in surface soil. The data suggest indirect effects of precipitation through influencing biomass production and litter decomposition processes that facilitate Hg accumulation in montane forest floor, rather than "cold trapping" effect that attribute Hg accumulation to lower temperatures (Blackwell & Driscoll, 2015; Gerson et al., 2017; Stankwitz et al., 2012; H. Zhang et al., 2013). The absence of rainfall Hg isotope signatures in forest surface soil is most likely caused by the shift of isotopic signals during the throughfall process contributed by the Hg washed away from the surface of vegetative biomass (e.g., leaves and branches). High-energy resolution X-ray absorption near-edge structure spectroscopy shows that up to 57% Hg in foliage is present as nanoparticulate Hg (SR)$_2$ that is less likely to be remobilized after deposition through litterfall to surface soil (Manceau et al., 2018). Atmospheric deposition of Hg^{2+} through precipitation and throughfall tends to have stronger mobility than litterfall Hg after deposition and therefore be diluted by Hg mass from other sources (e.g., geological Hg), removed by runoff, or reemitted into atmosphere after chemical/biological reduction (Amos et al., 2015; D. F. Grigal, 2002; Lindberg et al., 2007). Further studies are needed to verify these possible causes.

We found a significant correlation between precipitation and litterfall Hg input and a correlation between Hg pool size and C pool size in global-documented forest ecosystems (Figure 5a and 5b). The C content in the forest soil comes from decomposition of litter (X. Wang, Luo, et al., 2017). Results from SEM suggest that litterfall Hg deposition plays a predominant role in controlling Hg variation in soil. Thus, the correlation between Hg pool size and C pool size mainly reflects the variation of cumulative litterfall Hg deposition
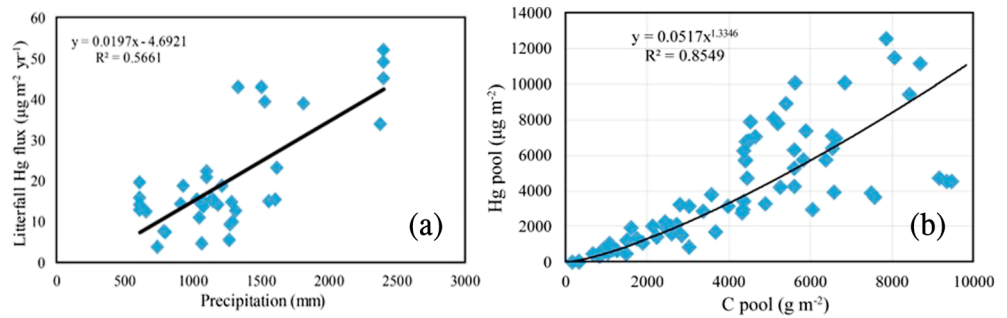
Figure 5. Global meta-analysis for (a) precipitation versus litterfall Hg deposition and (b) C pool versus Hg pool in forest soil. Data obtained from earlier references (Blackwell et al., 2014; Bringmark et al., 2013; Demers et al., 2007; Fisher & Wolfe, 2012; Fostier et al., 2000, 2015; X. W. Fu et al., 2010, 2015; Graydon et al., 2008; D. F. Grigal et al., 2000; Hultberg et al., 1995; Johnson et al., 2007; Juillerat et al., 2012; Larssen et al., 2008; Lee et al., 1998, 2000; John Munthe & Hultberg, 2004; J. Munthe et al., 1995; Niu et al., 2011; Rea et al., 1996, 2001, 2002; Risch et al., 2012; Schwesig & Matzner, 2000, 2001; Selvendiran et al., 2008; Sheehan et al., 2006; Silva et al., 2006; Slemr et al., 2015; St Louis et al., 2001; Teixeira et al., 2012; X. Wang, Lin, et al., 2016; Z. W. Wang et al., 2009; Zhou et al., 2013).

globally. Vegetation serves as an active "pump" to take up 1,000–1,200 Mg/year Hg^0 in global terrestrial ecosystems (X. Fu, Zhu, et al., 2016; X. Wang, Bao, et al., 2016). Though precipitation and soil moisture may not always be the limiting factor for vegetation net primary production (NPP) at the local scale (e.g., variation of NPP in rainfall forest), precipitation is the most important factor to explain the variability of the terrestrial NPP at the global scale (Del Grosso et al., 2008). Global climate warming is changing the spatial pattern of precipitation, thus likely poses an important and not-yet-quantified impact on global Hg biogeochemical cycling. Large-scale droughts have reduced 1.83 Pg C NPP in the Southern Hemisphere from 2000 through 2009, while the wetter and warmer trends in the Northern Hemisphere have increased 1.28 Pg C NPP (Zhao & Running, 2010). Given average ~50 ng/g C of Hg/C ratio in terrestrial ecosystems (M. Jiskra et al., 2018), we estimate total ~90 Mg decrease of vegetation Hg deposition in the Southern Hemisphere and ~75 Mg increase in the Northern Hemisphere from 2000 to 2009. A recent study indicates that atmospheric Hg^0 uptake by vegetation plays an important role in shaping the seasonal variations of atmospheric Hg^0 (M. Jiskra et al., 2018). Overall, the change of global precipitation thus has potential to perturb the present mass budgets of Hg cycling. Further studies are needed to more confidently quantify the impact of the precipitation changes on Hg accumulation in terrestrial ecosystems globally.

References

Agnan, Y., Le Dantec, T., Moore, C. W., Edwards, G. C., & Obrist, D. (2016). New constraints on terrestrial surface atmosphere fluxes of gaseous elemental mercury using a global database. *Environmental Science & Technology*, *50*(2), 507–524. https://doi.org/10.1021/acs.est.5b04013

Amos, H. M., Sonke, J. E., Obrist, D., Robins, N., Hagan, N., Horowitz, H. M., et al. (2015). Observational and modeling constraints on global anthropogenic enrichment of mercury. *Environmental Science & Technology*, *49*(7), 4036–4047. https://doi.org/10.1021/es5058665

Blackwell, B. D., & Driscoll, C. T. (2015). Deposition of mercury in forests along a montane elevation gradient. *Environmental Science & Technology*, *49*(9), 5363–5370. https://doi.org/10.1021/es505928w

Blackwell, B. D., Driscoll, C. T., Maxwell, J. A., & Holsen, T. M. (2014). Changing climate alters inputs and pathways of mercury deposition to forested ecosystems. *Biogeochemistry*, *119*(1–3), 215–228. https://doi.org/10.1007/s10533-014-9961-6

Blum, J. D., & Bergquist, B. A. (2007). Reporting of variations in the natural isotopic composition of mercury. *Analytical and Bioanalytical Chemistry*, *388*(2), 353–359. https://doi.org/10.1007/s00216-007-1236-9

Blum, J. D., Sherman, L. S., & Johnson, M. W. (2014). Mercury isotopes in earth and environmental sciences. *Annual Review of Earth and Planetary Sciences*, *42*(1), 249–269. https://doi.org/10.1146/annurev-earth-050212-124107

Breymeyer, A., Degorski, M., & Reed, D. (1997). Decomposition of pine-litter organic matter and chemical properties of upper soil layers: Transect studies. *Environmental Pollution*, *98*(3), 361–367. https://doi.org/10.1016/s0269-7491(97)00157-7

Bringmark, L., Lundin, L., Augustaitis, A., Beudert, B., Dieffenbach-Fries, H., Dirnböck, T., et al. (2013). Trace metal budgets for forested catchments in Europe-Pb, Cd, Hg, Cu and Zn. *Water, Air, & Soil Pollution*, *224*(4). https://doi.org/10.1007/s11270-013-1502-8

Chen, J. B., Hintelmann, H., Feng, X. B., & Dimock, B. (2012). Unusual fractionation of both odd and even mercury isotopes in precipitation from Peterborough, ON, Canada. *Geochimica et Cosmochimica Acta*, *90*, 33–46. https://doi.org/10.1016/j.gca.2012.05.005

Del Grosso, S., Parton, W., Stohlgren, T., Zheng, D., Bachelet, D., Prince, S., et al. (2008). Global potential net primary production predicted from vegetation class, precipitation, and temperature. *Ecology*, *89*(8), 2117–2126. https://doi.org/10.1890/07-0850.1

Demers, J. D., Blum, J. D., & Zak, D. R. (2013). Mercury isotopes in a forested ecosystem: Implications for air-surface exchange dynamics and the global mercury cycle. *Global Biogeochemical Cycles*, *27*, 222–238. https://doi.org/10.1002/gbc.20021

Demers, J. D., Driscoll, C. T., Fahey, T. J., & Yavitt, J. B. (2007). Mercury cycling in litter and soil in different forest types in the Adirondack region, New York, USA. *Ecological Applications*, *17*(5), 1341–1351. https://doi.org/10.1890/06-1697.1

Enrico, M., Le Roux, G., Heimburger, L.-E., van Beek, P., Souhaut, M., Chmeleff, J., & Sonke, J. E. (2017). Holocene atmospheric mercury levels reconstructed from peat bog mercury stable isotopes. *Environmental Science & Technology*, *51*(11), 5899–5906. https://doi.org/10.1021/acs.est.6b05804

Enrico, M., Le Roux, G., Maruszczak, N., Heimburger, L. E., Claustres, A., Fu, X. W., et al. (2016). Atmospheric mercury transfer to peat bogs dominated by gaseous elemental mercury dry deposition. *Environmental Science & Technology*, *50*(5), 2405–2412. https://doi.org/10.1021/acs.est.5b06058

Estrade, N., Carignan, J., Sonke, J. E., & Donard, O. F. X. (2010). Measuring Hg isotopes in bio-geo-environmental reference materials. *Geostandards and Geoanalytical Research*, *34*(1), 79–93. https://doi.org/10.1111/j.1751-908X.2009.00040.x

Fisher, L. S., & Wolfe, M. H. (2012). Examination of mercury inputs by throughfall and litterfall in the Great Smoky Mountains National Park. *Atmospheric Environment*, *47*, 554–559. https://doi.org/10.1016/j.atmosenv.2011.10.017

Fostier, A. H., Forti, M. C., Guimaraes, J. R. D., Melfi, A. J., Boulet, R., Santo, C. M. E., & Krug, F. J. (2000). Mercury fluxes in a natural forested Amazonian catchment (Serra do Navio, Amapa State, Brazil). *Science of the Total Environment*, *260*(1–3), 201–211. https://doi.org/10.1016/S0048-9697(00)00564-7

Fostier, A. H., Melendez-Perez, J. J., & Richter, L. (2015). Litter mercury deposition in the Amazonian rainforest. *Environmental Pollution*, *206*, 605–610. https://doi.org/10.1016/j.envpol.2015.08.010

Fu, X., Maruszczak, N., Wang, X., Gheusi, F., & Sonke, J. E. (2016). Isotopic composition of gaseous elemental mercury in the free troposphere of the Pic du Midi Observatory, France. *Environmental Science & Technology*, *50*(11), 5641–5650. https://doi.org/10.1021/acs.est.6b00033

Fu, X., Zhu, W., Zhang, H., Sommar, J., Yu, B., Yang, X., et al. (2016). Depletion of atmospheric gaseous elemental mercury by plant uptake at Mt. Changbai, Northeast China. *Atmospheric Chemistry and Physics*, *16*(20), 12,861–12,873. https://doi.org/10.5194/acp-16-12861-2016

Fu, X. W., Feng, X. B., Zhu, W. Z., Rothenberg, S., Yao, H., & Zhang, H. (2010). Elevated atmospheric deposition and dynamics of mercury in a remote upland forest of southwestern China. *Environmental Pollution*, *158*(6), 2324–2333. https://doi.org/10.1016/j.envpol.2010.01.032

Fu, X. W., Yang, X., Lang, X. F., Zhou, J., Zhang, H., Yu, B., et al. (2016). Atmospheric wet and litterfall mercury deposition at urban and rural sites in China. *Atmospheric Chemistry and Physics*, *16*(18), 11,547–11,562. https://doi.org/10.5194/acp-16-11547-2016

Fu, X. W., Zhang, H., Yu, B., Wang, X., Lin, C. J., & Feng, X. B. (2015). Observations of atmospheric mercury in China: A critical review. *Atmospheric Chemistry and Physics*, *15*(16), 9455–9476. https://doi.org/10.5194/acp-15-9455-2015

Gerson, J. R., Driscoll, C. T., Demers, J. D., Sauer, A. K., Blackwell, B. D., Montesdeoca, M. R., et al. (2017). Deposition of mercury in forests across a montane elevation gradient: Elevational and seasonal patterns in methylmercury inputs and production. *Journal of Geophysical Research: Biogeosciences*, *122*, 1922–1939. https://doi.org/10.1002/2016jg003721

Gratz, L. E., Keeler, G. J., Blum, J. D., & Sherman, L. S. (2010). Isotopic composition and fractionation of mercury in Great Lakes precipitation and ambient air. *Environmental Science & Technology*, *44*(20), 7764–7770. https://doi.org/10.1021/es100383w

Graydon, J. A., Louis, V. L. S., Hintelmann, H., Lindberg, S. E., Sandilands, K. A., Rudd, J. W. M., et al. (2008). Long-term wet and dry deposition of total and methyl mercury in the remote boreal ecoregion of Canada. *Environmental Science & Technology*, *42*(22), 8345–8351. https://doi.org/10.1021/es801056j

Grigal, D. F. (2002). Inputs and outputs of mercury from terrestrial watersheds: A review. *Environmental Reviews*, *10*(1), 1–39. https://doi.org/10.1139/a01-013

Grigal, D. F. (2003). Mercury sequestration in forests and peatlands: A review. *Journal of Environmental Quality*, *32*(2), 393–405. https://doi.org/10.2134/jeq2003.3930

Grigal, D. F., Kolka, R. K., Fleck, J. A., & Nater, E. A. (2000). Mercury budget of an upland-peatland watershed. *Biogeochemistry*, *50*(1), 95–109. https://doi.org/10.1023/A:1006322705566

Gustin, M. S., & Lindberg, S. E. (2000). Assessing the contribution of natural sources to the global mercury cycle: The importance of intercomparing dynamic flux measurements. *Fresenius Journal of Analytical Chemistry*, *366*(5), 417–422. https://doi.org/10.1007/s002160050085

Harmon, M. E., Silver, W. L., Fasth, B., Chen, H., Burke, I. C., Parton, W. J., et al., & Lidet (2009). Long-term patterns of mass loss during the decomposition of leaf and fine root litter: An intersite comparison. *Global Change Biology*, *15*(5), 1320–1338. https://doi.org/10.1111/j.1365-2486.2008.01837.x

Hultberg, H., Munthe, J., & Iverfeldt, A. (1995). Cycling of methyl mercury and mercury—Responses in the Forest roof catchment to 3 years of decreased atmospheric deposition. *Water, Air, & Soil Pollution*, *80*(1–4), 415–424. https://doi.org/10.1007/BF01189691

Jiskra, M., Sonke, J. E., Obrist, D., Bieser, J., Ebinghaus, R., Myhre, C. L., et al. (2018). A vegetation control on seasonal variations in global atmospheric mercury concentrations. *Nature Geoscience*, *11*(4), 244–250. https://doi.org/10.1038/s41561-018-0078-8

Jiskra, M., Wiederhold, J. G., Skyllberg, U., Kronberg, R. M., Hajdas, I., & Kretzschmar, R. (2015). Mercury deposition and re-emission pathways in boreal forest soils investigated with hg isotope signatures. *Environmental Science & Technology*, *49*(12), 7188–7196. https://doi.org/10.1021/acs.est.5b00742

Jiskra, M., Wiederhold, J. G., Skyllberg, U., Kronberg, R.-M., & Kretzschmar, R. (2017). Source tracing of natural organic matter bound mercury in boreal forest runoff with mercury stable isotopes. *Environmental Science: Processes & Impacts*, *19*(10), 1235–1248. https://doi.org/10.1039/C7EM00245A

Johnson, K. B., Haines, T. A., Kahl, J. S., Norton, S. A., Amirbahman, A., & Sheehan, K. D. (2007). Controls on mercury and methylmercury deposition for two watersheds in Acadia National Park, Maine. *Environmental Monitoring and Assessment*, *126*(1–3), 55–67. https://doi.org/10.1007/s10661-006-9331-5

Juillerat, J. I., Ross, D. S., & M. S. Bank (2012). Mercury in litterfall and upper soil horizons in forested ecosystems in Vermont, USA. *Environmental Toxicology and Chemistry*, *31*(8), 1720–1729. https://doi.org/10.1002/etc.1896

Keenan, R. J., Reams, G. A., Achard, F., Freitas, J. V. D., Grainger, A., & Lindquist, E. (2015). Dynamics of global forest area: Results from the FAO Global Forest Resources Assessment 2015. *Forest Ecology and Management*, *352*, 9–20. https://doi.org/10.1016/j.foreco.2015.06.014

Kritee, K., Barkay, T., & Blum, J. D. (2009). Mass dependent stable isotope fractionation of mercury during mer mediated microbial degradation of monomethylmercury. *Geochimica et Cosmochimica Acta*, *73*(5), 1285–1296. https://doi.org/10.1016/j.gca.2008.11.038

Kritee, K., Blum, J. D., Johnson, M. W., Bergquist, B. A., & Barkay, T. (2007). Mercury stable isotope fractionation during reduction of Hg (II) to Hg(0) by mercury resistant microorganisms. *Environmental Science & Technology*, *41*(6), 1889–1895. https://doi.org/10.1021/es062019t

Larssen, T., de Wit, H. A., Wiker, M., & Halse, K. (2008). Mercury budget of a small forested boreal catchment in southeast Norway. *Science of the Total Environment*, *404*(2–3), 290–296. https://doi.org/10.1016/j.scitotenv.2008.03.013

Lee, Y. H., Bishop, K. H., & Munthe, J. (2000). Do concepts about catchment cycling of methylmercury and mercury in boreal catchments stand the test of time? Six years of atmospheric inputs and runoff export at Svartberget, northern Sweden. *Science of the Total Environment*, *260*(1–3), 11–20. https://doi.org/10.1016/S0048-9697(00)00538-6

Lee, Y. H., Bishop, K. H., Munthe, J., Iverfeldt, A., Verta, M., Parkman, H., & Hultberg, H. (1998). An examination of current Hg deposition and export in Fenno-Scandian catchments. *Biogeochemistry*, *40*(2/3), 125–135. https://doi.org/10.1023/A:1005926321337

Lindberg, S., Bullock, R., Ebinghaus, R., Engstrom, D., Feng, X. B., Fitzgerald, W., et al. (2007). A synthesis of progress and uncertainties in attributing the sources of mercury in deposition. *Ambio*, *36*(1), 19–33. https://doi.org/10.1579/0044-7447(2007)36[19:ASOPAU]2.0.CO;2

Manceau, A., Wang, J. X., Rovezzi, M., Glatzel, P., & Feng, X. B. (2018). Biogenesis of mercury-sulfur nanoparticles in plant leaves from atmospheric gaseous mercury. *Environmental Science & Technology*, *52*(7), 3935–3948. https://doi.org/10.1021/acs.est.7b05452

Munthe, J., & Hultberg, H. (2004). *Mercury and methylmercury in runoff from a forested catchment—Concentrations, fluxes, and their response to manipulations*, (pp. 207–212). Netherlands: Springer.

Munthe, J., Hultberg, H., & Iverfeldt, A. (1995). Mechanisms of deposition of methylmercury and mercury to coniferous forests. *Water, Air, & Soil Pollution*, *80*(1–4), 363–371. https://doi.org/10.1007/BF01189686

Niu, Z. C., Zhang, X. S., Wang, Z. W., & Ci, Z. J. (2011). Field controlled experiments of mercury accumulation in crops from air and soil. *Environmental Pollution*, *159*(10), 2684–2689. https://doi.org/10.1016/j.envpol.2011.05.029

Obrist, D., Agnan, Y., Jiskra, M., Olson, C. L., Colegrove, D. P., Hueber, J., et al. (2017). Tundra uptake of atmospheric elemental mercury drives Arctic mercury pollution. *Nature*, *547*(7662), 201–204. https://doi.org/10.1038/nature22997

Obrist, D., Fain, X., & Berger, C. (2010). Gaseous elemental mercury emissions and CO_2 respiration rates in terrestrial soils under controlled aerobic and anaerobic laboratory conditions. *Science of the Total Environment*, *408*(7), 1691–1700. https://doi.org/10.1016/j.scitotenv.2009.12.008

Obrist, D., Kirk, J. L., Zhang, L., Sunderland, E. M., Jiskra, M., & Selin, N. E. (2018). A review of global environmental mercury processes in response to human and natural perturbations: Changes of emissions, climate, and land use. *Ambio*, *47*(2), 116–140. https://doi.org/10.1007/s13280-017-1004-9

Obrist, D., Pearson, C., Webster, J., Kane, T., Lin, C. J., Aiken, G. R., & Alpers, C. N. (2016). A synthesis of terrestrial mercury in the western United States: Spatial distribution defined by land cover and plant productivity. *Science of the Total Environment*, *568*, 522–535. https://doi.org/10.1016/j.scitotenv.2015.11.104

Pokharel, A. K., & Obrist, D. (2011). Fate of mercury in tree litter during decomposition. *Biogeosciences*, *8*(9), 2507–2521. https://doi.org/10.5194/bg-8-2507-2011

Rea, A. W., Keeler, G. J., & Scherbatskoy, T. (1996). The deposition of mercury in throughfall and litterfall in the lake champlain watershed: A short-term study. *Atmospheric Environment*, *30*(19), 3257–3263. https://doi.org/10.1016/1352-2310(96)00087-8

Rea, A. W., Lindberg, S. E., & Keeler, G. J. (2000). Assessment of dry deposition and foliar leaching of mercury and selected trace elements based on washed foliar and surrogate surfaces. *Environmental Science & Technology*, *34*(12), 2418–2425. https://doi.org/10.1021/es991305k

Rea, A. W., Lindberg, S. E., & Keeler, G. J. (2001). Dry deposition and foliar leaching of mercury and selected trace elements in deciduous forest throughfall. *Atmospheric Environment*, *35*(20), 3453–3462. https://doi.org/10.1016/S1352-2310(01)00133-9

Rea, A. W., Lindberg, S. E., Scherbatskoy, T., & Keeler, G. J. (2002). Mercury accumulation in foliage over time in two northern mixed-hardwood forests. *Water, Air, & Soil Pollution*, *133*(1/4), 49–67. https://doi.org/10.1023/A:1012919731598

Risch, M. R., DeWild, J. F., Krabbenhoft, D. P., Kolka, R. K., & Zhang, L. M. (2012). Litterfall mercury dry deposition in the eastern USA. *Environmental Pollution*, *161*, 284–290. https://doi.org/10.1016/j.envpol.2011.06.005

Rolison, J. M., Landing, W. M., Luke, W., Cohen, M., & Salters, V. J. M. (2013). Isotopic composition of species-specific atmospheric Hg in a coastal environment. *Chemical Geology*, *336*, 37–49. https://doi.org/10.1016/j.chemgeo.2012.10.007

Schwesig, D., & Matzner, E. (2000). Pools and fluxes of mercury and methylmercury in two forested catchments in Germany. *Science of the Total Environment*, *260*(1–3), 213–223. https://doi.org/10.1016/S0048-9697(00)00565-9

Schwesig, D., & Matzner, E. (2001). Dynamics of mercury and methylmercury in forest floor and runoff of a forested watershed in Central Europe. *Biogeochemistry*, *53*(2), 181–200. https://doi.org/10.1023/A:1010600600099

Selvendiran, P., Driscoll, C. T., Montesdeoca, M. R., & Bushey, J. T. (2008). Inputs, storage, and transport of total and methyl mercury in two temperate forest wetlands. *Journal of Geophysical Research*, *113*, G00C01. https://doi.org/10.1029/2008JG000739

Sheehan, K. D., Fernandez, I. J., Kahl, J. S., & Amirbahman, A. (2006). Litterfall mercury in two forested watersheds at Acadia National Park, Maine, USA. *Water, Air, & Soil Pollution*, *170*(1–4), 249–265. https://doi.org/10.1007/s11270-006-3034-y

Sherman, L. S., Blum, J. D., Keeler, G. J., Demers, J. D., & Dvonch, J. T. (2012). Investigation of local mercury deposition from a coal-fired power plant using mercury isotopes. *Environmental Science & Technology*, *46*(1), 382–390. https://doi.org/10.1021/es202793c

Silva, E. V., Machado, W., Oliveira, R. R., Sella, S. M., & Lacerda, L. D. (2006). Mercury deposition through litterfall in an Atlantic Forest at Ilha Grande, southeast Brazil. *Chemosphere*, *65*(11), 2477–2484. https://doi.org/10.1016/j.chemosphere.2006.04.053

Slemr, F., Angot, H., Dommergue, A., Magand, O., Barret, M., Weigelt, A., et al. (2015). Comparison of mercury concentrations measured at several sites in the Southern Hemisphere. *Atmospheric Chemistry and Physics*, *15*(6), 3125–3133. https://doi.org/10.5194/acp-15-3125-2015

Smith, C. N., Kesler, S. E., Blum, J. D., & Rytuba, J. J. (2008). Isotope geochemistry of mercury in source rocks, mineral deposits and spring deposits of the California Coast Ranges, USA. *Earth and Planetary Science Letters*, *269*(3–4), 398–406.

Sonke, J. E. (2011). A global model of mass independent mercury stable isotope fractionation. *Geochimica et Cosmochimica Acta*, *75*(16), 4577–4590. https://doi.org/10.1016/j.gca.2011.05.027

Sprovieri, F., Pirrone, N., Bencardino, M., D'Amore, F., Angot, H., Barbante, C., et al. (2017). Five-year records of mercury wet deposition flux at GMOS sites in the Northern and Southern hemispheres. *Atmospheric Chemistry and Physics*, *17*(4), 2689–2708. https://doi.org/10.5194/acp-17-2689-2017

Sprovieri, F., Pirrone, N., Bencardino, M., D'Amore, F., Carbone, F., Cinnirella, S., et al. (2016). Atmospheric mercury concentrations observed at ground-based monitoring sites globally distributed in the framework of the GMOS network. *Atmospheric Chemistry and Physics Discussions*, 1–32. https://doi.org/10.5194/acp-2016-466

St Louis, V. L., Rudd, J. W. M., Kelly, C. A., Hall, B. D., Rolfhus, K. R., Scott, K. J., et al. (2001). Importance of the forest canopy to fluxes of methyl mercury and total mercury to boreal ecosystems. *Environmental Science & Technology*, *35*(15), 3089–3098. https://doi.org/10.1021/es001924p

Stankwitz, C., Kaste, J. M., & Friedland, A. J. (2012). Threshold increases in soil lead and mercury from tropospheric deposition across an elevational gradient. *Environmental Science & Technology*, *46*(15), 8061–8068. https://doi.org/10.1021/es204208w

Strauss, S. L., Garcia-Pichel, F., & Day, T. A. (2012). Soil microbial carbon and nitrogen transformations at a glacial foreland on Anvers Island, Antarctic Peninsula. *Polar Biology*, *35*(10), 1459–1471. https://doi.org/10.1007/s00300-012-1184-5

Sun, G., Sommar, J., Feng, X., Lin, C.-J., Ge, M., Wang, W., et al. (2016). Mass-dependent and -independent fractionation of mercury isotope during gas-phase oxidation of elemental mercury vapor by atomic Cl and Br. *Environmental Science & Technology*, *50*(17), 9232–9241. https://doi.org/10.1021/acs.est.6b01668

Teixeira, D. C., Montezuma, R. C., Oliveira, R. R., & Silva, E. V. (2012). Litterfall mercury deposition in Atlantic forest ecosystem from SE-Brazil. *Environmental Pollution*, *164*, 11–15. https://doi.org/10.1016/j.envpol.2011.10.032

Wang, X., Bao, Z., Lin, C.-J., Yuan, W., & Feng, X. (2016). Assessment of global mercury deposition through Litterfall. *Environmental Science & Technology*, *50*(16), 8548–8557. https://doi.org/10.1021/acs.est.5b06351

Wang, X., Lin, C.-J., Lu, Z., Zhang, H., Zhang, Y., & Feng, X. (2016). Enhanced accumulation and storage of mercury on subtropical evergreen forest floor: Implications on mercury budget in global forest ecosystems. *Journal of Geophysical Research: Biogeosciences*, *121*, 2096–2109. https://doi.org/10.1002/2016jg003446

Wang, X., Luo, J., Yin, R., Yuan, W., Lin, C.-J., Sommar, J., et al. (2017). Using mercury isotopes to understand mercury accumulation in the montane forest floor of the Eastern Tibetan Plateau. *Environmental Science & Technology*, *51*(2), 801–809. https://doi.org/10.1021/acs.est.6b03806

Wang, X., Yuan, W., & Feng, X. (2017). Global review of mercury biogeochemical processes in forest ecosystems. *Progress in Chemistry*, *29*(9), 970–980. https://doi.org/10.7536/PC170343.

Wang, Z. W., Zhang, X. S., Xiao, J. S., Zhijia, C., & Yu, P. Z. (2009). Mercury fluxes and pools in three subtropical forested catchments, southwest China. *Environmental Pollution*, *157*(3), 801–808. https://doi.org/10.1016/j.envpol.2008.11.018

Woerndle, G. E., Tsui, M. T. K., Sebestyen, S. D., Blum, J. D., Nie, X. P., & Kolka, R. K. (2018). New insights on ecosystem mercury cycling revealed by stable isotopes of mercury in water flowing from a headwater peatland catchment. *Environmental Science & Technology*, *52*(4), 1854–1861. https://doi.org/10.1021/acs.est.7b04449

Yang, Z., & Yang, X. D. (2011). Characteristics of floor litter and soil arthropod community in different types of subtropical forest in Ailao Mountain of YunnanSouthwest China. *Chinese Journal of Applied Ecology*, *22*(11), 3011–3020.

Yin, R. S., Feng, X. B., Foucher, D., Shi, W. F., Zhao, Z. Q., & Wang, J. (2010). High precision determination of mercury isotope ratios using online mercury vapor generation system coupled with multi-collector inductively coupled plasma-mass spectrometry. *Chinese Journal of Analytical Chemistry*, *38*(7), 929–934. https://doi.org/10.1016/S1872-2040(09)60055-4

Yin, R. S., X. B. Feng, J. P. Hurley, D. P. Krabbenhoft, R. F. Lepak, S. C. Kang, et al. (2016), Historical records of mercury stable isotopes in sediments of Tibetan Lakes, Sci Rep-Uk, 6.

Yu, B., Fu, X., Yin, R., Zhang, H., Wang, X., Lin, C. J., et al. (2016). Isotopic composition of atmospheric mercury in China: New evidence for sources and transformation processes in air and in vegetation. *Environmental Science & Technology*, *50*(17), 9262–9269. https://doi.org/10.1021/acs.est.6b01782

Yuan, S., Zhang, Y., Chen, J., Kang, S., Zhang, J., Feng, X., et al. (2015). Large Variation of Mercury Isotope Composition During a Single Precipitation Event at Lhasa City, Tibetan Plateau, China. *Procedia Earth and Planetary Science*, *13*, 282–286. https://doi.org/10.1016/j.proeps.2015.07.066

Zhang, D., Hui, D., Luo, Y., & Zhou, G. (2008). Rates of litter decomposition in terrestrial ecosystems: Global patterns and controlling factors. *Journal of Plant Ecology*, *1*(2), 85–93. https://doi.org/10.1093/jpe/rtn002

Zhang, H., Fu, X. W., Lin, C. J., Shang, L. H., Zhang, Y. P., Feng, X. B., & Lin, C. (2016). Monsoon-facilitated characteristics and transport of atmospheric mercury at a high-altitude background site in southwestern China. *Atmospheric Chemistry and Physics*, *16*(20), 13,131–13,148. https://doi.org/10.5194/acp-16-13131-2016

Zhang, H., R. S. Yin, X. B. Feng, J. Sommar, C. W. N. Anderson, A. Sapkota, et al. (2013), Atmospheric mercury inputs in montane soils increase with elevation: Evidence from mercury isotope signatures, Sci Rep-Uk, 3.

Zhao, M. S., & Running, S. W. (2010). Drought-induced reduction in global terrestrial net primary production from 2000 through 2009. *Science*, *329*(5994), 940–943. https://doi.org/10.1126/science.1192666

Zheng, W., Obrist, D., Weis, D., & Bergquist, B. A. (2016). Mercury isotope compositions across North American forests. *Global Biogeochemical Cycles*, *30*, 1475–1492. https://doi.org/10.1002/2015GB005323

Zhou, J., Feng, X. B., Liu, H. Y., Zhang, H., Fu, X. W., Bao, Z. D., et al. (2013). Examination of total mercury inputs by precipitation and litterfall in a remote upland forest of Southwestern China. *Atmospheric Environment*, *81*, 364–372. https://doi.org/10.1016/j.atmosenv.2013.09.010